

## Structure of a *Bacillus halmapalus* family 13 $\alpha$ -amylase, BHA, in complex with an acarbose-derived nonasaccharide at 2.1 Å resolution

Gideon J. Davies,<sup>a\*</sup> A. Marek Brzozowski,<sup>a</sup> Zbigniew Dauter,<sup>a‡</sup> Michael D. Rasmussen,<sup>b</sup> Torben V. Borchert<sup>b</sup> and Keith S. Wilson<sup>a</sup>

<sup>a</sup>Department of Chemistry, University of York, England, and <sup>b</sup>Novozymes A/S, Denmark

<sup>‡</sup> Current address: Argonne National Laboratory, USA.

Correspondence e-mail: [davies@ysbl.york.ac.uk](mailto:davies@ysbl.york.ac.uk)

Received 16 September 2004  
Accepted 25 October 2004

**PDB Reference:** BHA–nonasaccharide complex, 1w9x, r1w9xsf.

The enzymatic digestion of starch by  $\alpha$ -amylases is one of the key biotechnological reactions of recent times. In the search for industrial biocatalysts, the family GH13  $\alpha$ -amylase BHA from *Bacillus halmapalus* has been cloned and expressed. The three-dimensional structure at 2.1 Å resolution has been determined in complex with the (pseudo)tetrasaccharide inhibitor acarbose. Acarbose is found bound as a nonasaccharide transglycosylation product spanning the –6 to +3 subsites. Careful inspection of electron density suggests that the bound ligand could not have been formed through successive transglycosylations of acarbose and must also have featured maltose or maltooligosaccharides as an acceptor.

### 1. Introduction

The  $\alpha$ -amylase-catalysed hydrolysis of starch is one of the key industrial biotransformations of modern times. These enzymes (1,4- $\alpha$ -glucan 4-glucanohydrolases; EC 3.2.1.1) catalyse the hydrolysis of the internal  $\alpha$ -1,4 linkages in amylose and amylopectin.  $\alpha$ -Amylases are predominantly found in a sequence-related family of enzymes (now numbering over 1700 members) termed glycoside hydrolase family GH13 (Coutinho & Henrissat, 1999) or the  $\alpha$ -amylase superfamily (Janecek *et al.*, 1997, 2003; MacGregor *et al.*, 2001; Svensson, 1994). Three-dimensional structures are known for over 40 family members, all of which are composed of a central ( $\beta/\alpha$ )<sub>8</sub> catalytic domain termed domain A within which an insertion between  $\beta$ -3 and  $\alpha$ -3 forms an excursion termed domain B. The active centre and substrate-binding crevice lie at the interface of the A and B domains.

$\alpha$ -Amylases are 'retaining' glycoside hydrolases: the configuration of the anomeric carbon is retained (as opposed to inverted) during hydrolysis. All  $\alpha$ -amylase family members thus perform catalysis *via* a covalent glycosyl-enzyme intermediate whose formation and breakdown occurs *via* oxocarbenium-ion-like transition states (reviewed in Davies *et al.*, 1997; Zechel & Withers, 1999, 2000). Enzyme inhibition through mimicry of this transition state is medically relevant, with compounds such as miglitol and acarbose being used in the treatment of type II diabetes for the inhibition of the intestinal  $\alpha$ -glucosidase. The pseudo-tetrasaccharide acarbose also finds frequent use in the structural dissection of GH13 protein–ligand interactions by X-ray crystallography, where it has frequently been observed as an extended species with a degree of polymerization greater than the four of the starting material. Such species are formed through enzymatic transglycosylation (Fig. 1*a*), in which the covalent glycosyl-enzyme intermediate is intercepted by another sugar, rather than water, to form a longer and tighter binding inhibitor whose length generally reflects the number of subsites of the enzyme in question (examples include Aghajari *et al.*, 2002; Brzozowski & Davies, 1997; Brzozowski *et al.*, 2000; Mosi *et al.*, 1998; Qian *et al.*, 1994).

$\alpha$ -Amylases find widespread industrial use, predominantly for the conversion of corn starch, ultimately to high fructose syrups, and as an additive to laundry detergents, but also in the baking and pharmaceutical industries (for a review, see Nielsen & Borchert, 2000). Industrial concerns are always screening for new enzymes with appropriate properties. In detergent applications, for example, amylases must withstand highly alkaline pH values (up to pH 10.5; Nielsen & Borchert, 2000), with the added complication that detergents formulations contain proteases and are often significantly

oxidizing. In this context, we present here the structure of a GH13  $\alpha$ -amylase, BHA, from the bacteria *Bacillus halmapalus*. The enzyme was isolated from an alkaliphilic *Bacillus* species and indeed displays activity at an elevated pH (above 9), making it a candidate for industrial applications. The structure of BHA at 2.1 Å resolution reveals the canonical  $\alpha$ -amylase structure with A, B and C domains comprising (approximately) residues 5–110/212–398, 111–211 and 399–484, respectively. Unusually, the structure crystallized in the presence of acarbose reveals a nonasaccharide species that cannot simply be derived from the transglycosylation of acarbose but must instead involve successive maltose units or maltooligosaccharides as acceptors for the elongation process.

## 2. Experimental

### 2.1. Crystallization and data collection

Recombinant *B. halmapalus*  $\alpha$ -amylase BHA was provided by Novozymes A/S. Briefly, the gene encoding BHA was isolated from the alkaliphilic *Bacillus* species *B. halmapalus* (Nielsen *et al.*, 1995) and cloned into a *B. subtilis* expression vector derived from pUB110 (McKenzie *et al.*, 1986). The resulting *B. subtilis* strain was grown in a complex soy-meal media from which the amylase was purified.

The hanging-drop vapour-diffusion method and in-house screens were used in a search for the crystallization conditions. Crystals in complex with acarbose were grown from enzyme solution at 30 mg ml<sup>-1</sup> in 50 mM imidazole, 5 mM CaCl<sub>2</sub>, 25 mM acarbose pH 7.5 mixed in a 1:1 ratio with well solution consisting of 0.1 M imidazole pH 7.5, 100 mM maltose, 5 mM CaCl<sub>2</sub> and with 18% (w/v) monomethylether polyethylene glycol 5K as precipitant. Data were collected at room temperature using an R-Axis II image plate together with a Cu rotating anode and utilizing long focusing-mirror optics (Yale/Molecular Structure Corporation). 113° of data were collected with an oscillation range of 1° per image. Data were processed and reduced using the DENZO and SCALEPACK programs (Otwinowski & Minor, 1997). All further calculations used

**Table 1**

Data and structure-quality statistics for the *B. halmapalus*  $\alpha$ -amylase BHA at 2.1 Å resolution.

Values in parentheses are for the outer resolution shell.

Data quality	
Resolution (Å)	15–2.1 (2.2–2.1)
$R_{\text{merge}}$	0.091 (0.337)
Mean $I/\sigma(I)$	13.6 (4.8)
Completeness (%)	99.7 (98.9)
Multiplicity	3.6 (3.5)
Refinement	
No. of protein atoms	4301
No. of metal ions	3 Ca <sup>2+</sup> , 1 Na <sup>+</sup>
No. of oligosaccharide atoms	389
No. of solvent waters	290
Resolution used in refinement (Å)	15–2.1
$R_{\text{cryst}}$	0.15
$R_{\text{free}}$	0.20
R.m.s. deviation 1–2 bonds (Å)	0.017
R.m.s. deviation angles (°)	0.131
Average main-chain $B$ (Å <sup>2</sup> )	18
Average side-chain $B$ (Å <sup>2</sup> )	19
Average oligosaccharide $B$ (Å <sup>2</sup> )	30
Average solvent $B$ (Å <sup>2</sup> )	31

the CCP4 suite of programs (Collaborative Computational Project Number 4, 1994) unless otherwise stated.

### 2.2. Structure solution and refinement

The BHA–acarbose structure was solved by molecular replacement using *AMoRe* (Navaza & Saludjian, 1997) with the native BA2 amylase (PDB code 1e3x) as the search model (Brzozowski *et al.*, 2000). BA2 is a chimera consisting of residues 1–300 from a *B. amyloliquefaciens*  $\alpha$ -amylase and 301–483 from the corresponding *B. licheniformis* enzyme. 5% of the reflections were set aside for cross-validation (Brünger, 1992) and were used to monitor various refinement strategies such as geometric and temperature-factor restraint values, the insertion of solvent water and as the basis for maximum-likelihood refinement using the *REFMAC* program (Murshudov *et al.*, 1997). As all observed data from 15 Å resolution

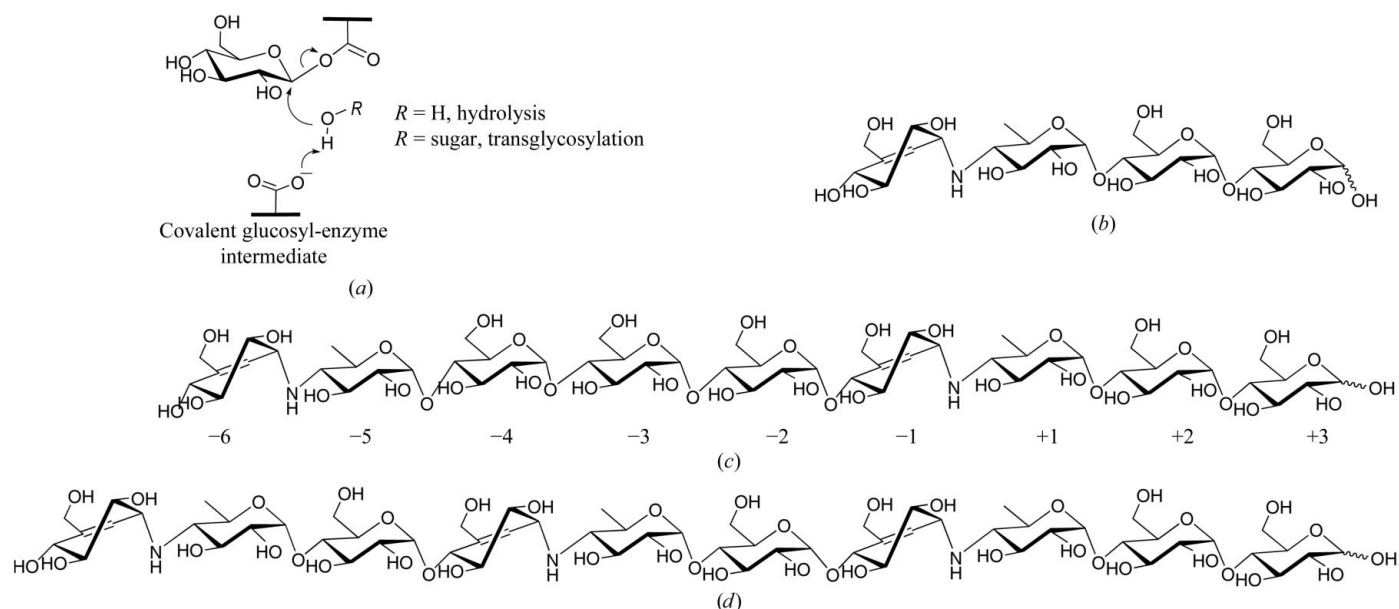


**Figure 1**

(a) The covalent glycosyl-enzyme intermediate of a retaining glycosidase is normally intercepted by water. Under some circumstances, it is instead intercepted by another sugar in a transglycosylation reaction; such a mechanism gives rise to the many elongated forms of acarbose seen in amylase structures. (b) The structure of the pseudo-tetrasaccharide inhibitor acarbose. (c) The nonasaccharide observed in BHA (this work) and (d) that previously observed on the BA2  $\alpha$ -amylase (Brzozowski *et al.*, 2000).

were employed in the refinement, a low-resolution bulk-solvent mask correction was applied as implemented in *REFMAC*. Water molecules were added in an automated manner using *ARP* (Lamzin & Wilson, 1993) and verified by manual inspection. Coordinates and observed structure-factor amplitudes for the protein structure described in this paper have been deposited with the PDB. Model coordinates for the acarbose-derived nonasaccharide were generated in *QUANTA* (Accelrys, San Diego, USA).

### 3. Results and discussion

#### 3.1. Structure of the *B. halmapalus* BHA $\alpha$ -amylase

Crystals of BHA belong to space group  $P2_12_12_1$ , with unit-cell parameters  $a = 48.2$ ,  $b = 75.9$ ,  $c = 155.2$  Å,  $\alpha = \beta = \gamma = 90^\circ$ . There is a

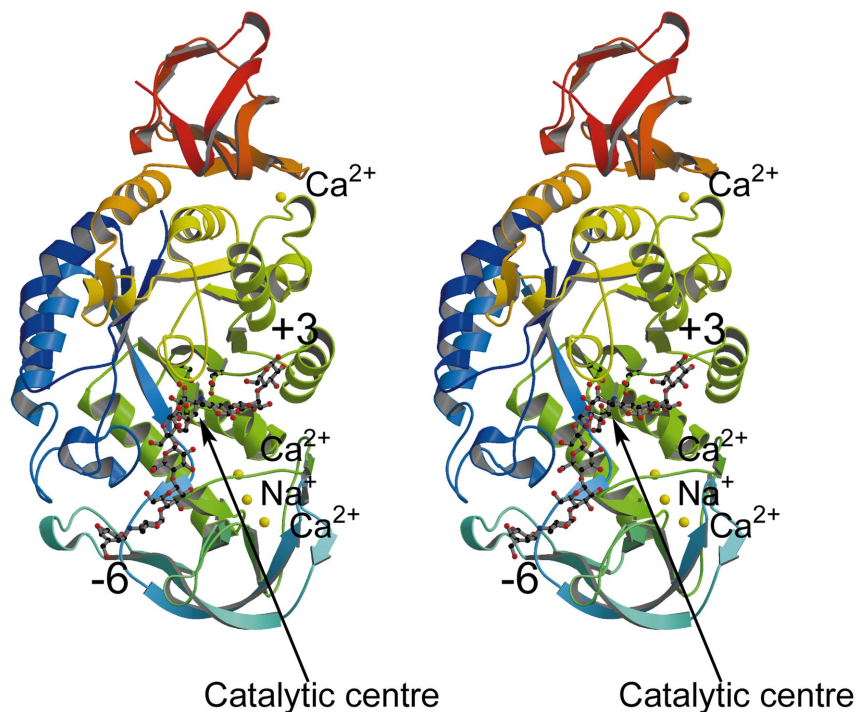


**Figure 2**  
Three-dimensional structure of the *Bacillus* sp. BHA  $\alpha$ -amylase with bound ligand in ball-and-stick representation and metal ions shown as spheres (drawn with *MOLSCRIPT*; Kraulis, 1991). The acarbose-derived nonasaccharide binds in the  $-6$  to  $+3$  subsites.

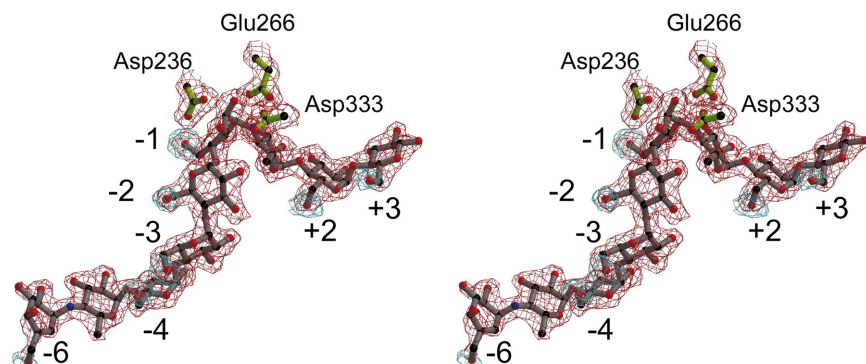


**Figure 3**  
Observed electron density for the acarbose-derived nonasaccharide bound to the *Bacillus* sp. BHA  $\alpha$ -amylase at  $2.1$  Å resolution. The maps shown are a maximum-likelihood (Murshudov *et al.*, 1997) and  $\sigma_A$  (Read, 1986) weighted  $2F_{\text{obs}} - F_{\text{calc}}$  synthesis contoured at  $0.3 \text{ e \AA}^{-3}$  (approximately  $1\sigma$ ) in red and an  $F_{\text{obs}} - F_{\text{calc}}$  difference map (at  $3\sigma$ ) in which the O6 atoms were not included in the refinement or phase calculation in blue. The difference map clearly reveals density for O6 atoms in the  $-6$ ,  $-4$ ,  $-3$ ,  $-2$ ,  $-1$ ,  $+1$ ,  $+2$ , and  $+3$  sites (see Fig. 1c for interpretation and comparison).

single molecule of BHA in the asymmetric unit. Structure solution with the known BA2 chimeric  $\alpha$ -amylase (Brzozowski *et al.*, 2000), which displays 70% sequence identity to BHA, proceeded without problem. The final BHA model, at  $2.1$  Å resolution, has a crystallographic  $R$  value of 0.15, with a corresponding  $R_{\text{free}}$  of 0.20 using all observed data between  $15$  and  $2.1$  Å. A single residue, Tyr152, has main-chain  $\varphi/\psi$  angles in a 'forbidden' region of the Ramachandran plot, but the density (not shown) is unambiguous. Data and model-quality parameters are shown in Table 1.

The three-dimensional structure of BHA (Fig. 2) is extremely similar to the closely related chimeric BA2 (Brzozowski *et al.*, 2000), a feature that was utilized in the molecular-replacement structure determination. Both the overall structure and unusual  $\text{Ca}^{2+}/\text{Na}^{+}$  binding sites are essentially identical to those of BA2. In both cases,  $\text{Ca}^{2+}/\text{Na}^{+}$  identification was based upon electron-density levels (and consequent atomic  $B$  value; 8, 9, 13 and  $8 \text{ \AA}^2$  for the three  $\text{Ca}^{2+}$  and single  $\text{Na}^{+}$ , respectively) and coordination geometry (heptavalent and hexavalent for the  $\text{Ca}^{2+}$  and tetravalent for  $\text{Na}^{+}$ ). In contrast to BA2, the initial  $2F_{\text{obs}} - F_{\text{calc}}$  electron-density maps (and  $F_{\text{obs}} - F_{\text{calc}}$  difference density maps) clearly revealed a bound nonasaccharide species that must have been formed by a different transglycosylation route to that observed previously for related enzymes.

#### 3.2. Identity of the bound ligand

In the initial electron-density maps, it was clear that the pseudotetrasaccharide inhibitor acarbose (Fig. 1b) was bound as an apparent nonasaccharide species (Figs. 1c and 3). Acarbose in complexes of  $\alpha$ -amylases is indeed frequently observed as longer species. These extended species are most likely to arise from transglycosylation. Transglycosylation involves the formation of a covalent glycosyl-enzyme intermediate and its subsequent interception, not by water but by a further sugar molecule, resulting in extension (Fig. 1a.) In this way, longer oligosaccharides build up whose formation, although thermodynamically disfavoured, is kinetically driven. In the case of acarbose, such ligands become even better inhibitors as they span a greater number of subsites, eventually inhibiting the enzyme and yielding stable complexes for X-ray crystallography.

In BHA-acarbose the nonasaccharide spans the subsites  $-6$  to  $+3$ . As with BA2 (Brzozowski *et al.*, 2000), particular care was taken during the refinement of the acarbose-derived nonasaccharide in BHA to identify potential half-chair rings or 6-deoxy sugars. All O6 hydroxyls were omitted from refinement, no torsion-angle restraints were initially applied to the pyranosides and  $2F_{\text{obs}} - F_{\text{calc}}$  electron-density maps were calculated using phases generated prior to the incorporation of the ligand. This refinement and unbiased electron-density maps reveal that glucose units in the  $-4$ ,  $-3$ ,  $-2$ ,  $-1$ ,  $+1$ ,  $+2$  and  $+3$  subsites all possess their O6 hydroxyl substi-

tuent. The -5 sugar may well be a deoxy sugar and may be indicative of the acarbose moiety at the reducing end (that is demanded by all schemes for transglycosylation), whilst the -6 subsite is partially disordered, making assignment ambiguous (Fig. 1c). Of the well ordered sugars, only the -1 subsite sugar refines to a half-chair conformation when torsion-angle restraints are lifted.

The presence of glucopyranosides (and not 6-deoxy sugars) in the -4 to -1 subsites suggests that the ligand observed in the BHA structure was not formed by the same mechanism as that observed in the comparable BA2 complex with an acarbose-derived decasaccharide (see Fig. 1d for comparison). In BA2, the acarbose-derived decasaccharide was clearly formed by successive transglycosylations of acarbose, yielding a species in which every third sugar was a deoxy moiety and each of these was adjacent to an unsaturated species in half-chair conformation (Brzozowski *et al.*, 2000). The BHA complex features 'acarbose' in the -1 to +3 subsites, as expected, yet sugars in the -4 to -2 subsites all appear to be  $\alpha$ -1,4-linked D-glucopyranosides, thus displaying both a hydroxymethyl substituent and possessing  ${}^4C_1$  chair conformation. The observed nonasaccharide thus cannot have been made by successive transglycosylations of acarbose. Indeed, this species could only arise following the initial formation of a covalent intermediate from acarbose, followed by a limited number of successive transglycosylations with maltose (or contaminating longer maltooligosaccharides) from the crystallization liquor and a final 'capping' with a second molecule of acarbose. Given that both the initiation of extension and its completion involve acarbose, the newly formed ligand has an acarbose moiety at both its reducing and non-reducing ends. Whilst such a scheme is unusual, BHA in a crystal will necessarily select for the transglycosylation species that binds most tightly and its observation is thus in keeping with extended species seen in other systems.

#### 4. Summary

The alkaliphilic pH profile of the enzyme and the relatively high catalytic rate makes BHA an interesting candidate for industrial uses such as an additive to laundry and automated dishwashing detergents in order to aid the removal of starch-containing stains. Here, we reveal its three-dimensional structure in complex with a novel acarbose-derived nonasaccharide. The bound ligand not only unveils the subsite interactions but also reveals yet another different transglycosylation scheme for acarbose: one that involves the incorpora-

tion of maltose or contaminating maltooligosaccharides during the elongation process.

The authors would like to thank Novozymes A/S and the BBSRC for continued funding. GJD is a Royal Society University Research Fellow.

#### References

- Aghajari, N., Roth, M. & Haser, R. (2002). *Biochemistry*, **41**, 4273–4280.
- Brünger, A. T. (1992). *Nature (London)*, **355**, 472–475.
- Brzozowski, A. M. & Davies, G. J. (1997). *Biochemistry*, **36**, 10837–10845.
- Brzozowski, A. M., Lawson, D. M., Turkenburg, J. P., Bisgaard-Frantzen, H., Svendsen, A., Borchert, T. V., Dauter, Z., Wilson, K. S. & Davies, G. J. (2000). *Biochemistry*, **39**, 9099–9107.
- Collaborative Computational Project, Number 4 (1994). *Acta Cryst.* **D50**, 760–763.
- Coutinho, P. M. & Henrissat, B. (1999). *Recent Advances in Carbohydrate Engineering*, edited by H. J. Gilbert, G. J. Davies, B. Svensson & B. Henrissat, pp. 3–12. Cambridge: Royal Society of Chemistry.
- Davies, G. J., Sinnott, M. L. & Withers, S. G. (1997). *Comprehensive Biological Catalysis*, Vol. 1, edited by M. L. Sinnott, pp. 119–20. London: Academic Press.
- Janecek, S., Svensson, B. & Henrissat, B. (1997). *J. Mol. Evol.* **45**, 322–331.
- Janecek, S., Svensson, B. & MacGregor, E. A. (2003). *Eur. J. Biochem.* **270**, 635–645.
- Kraulis, P. J. (1991). *J. Appl. Cryst.* **24**, 946–950.
- Lamzin, V. S. & Wilson, K. S. (1993). *Acta Cryst.* **D49**, 129–147.
- MacGregor, E. A., Janecek, S. & Svensson, B. (2001). *Biochim. Biophys. Acta*, **1546**, 1–20.
- McKenzie, T., Hoshino, T., Tanaka, T. & Sueoka, N. (1986). *Plasmid*, **15**, 93–103.
- Mosi, R., Sham, H., Uitdehaag, J. C., Ruiterkamp, R., Dijkstra, B. W. & Withers, S. G. (1998). *Biochemistry*, **37**, 17192–17198.
- Murshudov, G. N., Vagin, A. A. & Dodson, E. J. (1997). *Acta Cryst.* **D53**, 240–255.
- Navaza, J. & Saludjian, P. (1997). *Methods Enzymol.* **276**, 581–594.
- Nielsen, J. E. & Borchert, T. V. (2000). *Biochim. Biophys. Acta*, **1543**, 253–274.
- Nielsen, P., Fritze, D. & Priest, F. G. (1995). *Microbiology*, **141**, 1745–1761.
- Otwinowski, Z. & Minor, W. (1997). *Methods Enzymol.* **276**, 307–326.
- Qian, M., Haser, R., Buisson, G., Duée, E. & Payan, F. (1994). *Biochemistry*, **33**, 6284–6294.
- Read, R. J. (1986). *Acta Cryst.* **A42**, 140–149.
- Svensson, B. (1994). *Plant Mol. Biol.* **25**, 141–157.
- Zechel, D. & Withers, S. G. (1999). *Comprehensive Natural Products Chemistry*, Vol. 5, edited by D. Barton, K. Nakanishi & C. D. Poulter, pp. 279–314. Amsterdam: Elsevier.
- Zechel, D. L. & Withers, S. G. (2000). *Acc. Chem. Rev.* **33**, 11–18.